FRP-STEEL-CONCRETE HYBRID MEMBER USING WET-BONDING TECHNIQUE

Zhishen Wu*, Kentaro Iwashita*, Haitang Zhu**
***Ibaraki University, ** Zhengzhou University**

Keywords: *FRP sheets, wet bonding, RC beam, hybrid system*

Abstract

A novel type of fiber reinforced polymer (FRP)-steel-concrete hybrid structure is proposed as a type of new construction. The hybrid structure is composed of an externally bonded hybrid FRP shell and a concrete core reinforced with internal steel reinforcements. The FRP shell includes high modulus type and high strength type of carbon FRP (MC and SC) sheets and glass FRP (EG) sheets with high ductility. Hybrid FRP sheets were axially and wetly bonded to the bottom surface of the concrete core to carry tensile load; while additional EG sheets were hoop-directionally wrapped to bear the shear load. The external FRP shell also provided the concrete core and steel rebars with an effective potential protection against corrosion. A series of 4-point bending experiments were carried out to confirm the structural performances of the proposed structures. Furthermore, the effectiveness of the wet-bonding method was also verified.

1 Introduction

Fiber Reinforced Polymer (FRP) plates or sheets have been increasingly used in recent years for the repair and rehabilitation of existing structures due to their high specific strength, high durability, excellent corrosion resistance, ease of installation, and tremendous design flexibility etc. The FRP-concrete composite design concept for a new construction was explored in the early 1990's for an E-glass fiber reinforced polymer box beam with a thin layer of concrete on the compression flange and a thinner layer of MC and/or SC on the tension flange [1]. The new hybrid FRP-concrete structural systems take advantage of the strengths inherent in each of the constituents and have been recently proposed for flexural applications [2-5]. Studies [1,5] have shown that interface debonding was the weak link that promoted premature failure and reduced the load-carrying capacity. To insure a composite action between the FRP shell and the concrete, a pultruded channel section filled with plain concrete was developed for an industrial floor decking application using shear keys [6], and a pultruded box beam that was chemically bonded to 100mm-thick pre-cast concrete slabs in the compression zone. The adhesive bond was demonstrated to be better than the mechanical bond using shear keys in FRP-concrete structures [7]. In our previous study, the authors proposed the hybrid FRP-concrete structural system with externally bonding several types of FRPs with various specific properties. It was experimentally confirmed that integrative flexural performances, including load carrying capacity, stiffness, and ductility could be thoroughly realized [8]. However, the debonding of FRPs is one of the serious problems. Moreover, the externally bonding process needs a long time and a high cost. On the basis of these studies, a new FRP-reinforced concrete composite system is proposed, in this study, as one type of innovative flexural structures with wet-bonding method. To effectively use these expensive composites as external reinforcements, the hybrid system utilizes the best combination of various types of continuous fibers in the terms of their mechanical behavior and cost performance. In addition, instead of using conventional interior shear connectors at the FRP-concrete interface, a wet-bonding method is used in the proposed innovative system in order to insure the composite effect between the FRP shell and the concrete. Moreover, the hybrid shell can be also considered in terms of its ability to protect the inner concrete core and steel rebars from environmental corrosion. An experimental program using 4-point bending girder specimens with various combinations of longitudinal reinforcements and control RC beams for comparison was investigated. The flexural behaviors of hybrid FRP-steel-concrete girders were studied, and also compared with conventional reinforced concrete beams.

2 FRP-steel-concrete hybrid member with the wet-bonding method

Existing FRP-concrete composite structures are normally strengthened with a single type of fiber composite and used shear connectors at the interface of the FRP and concrete. However, it is difficult to meet the required integrated structural performances for both serviceability and ultimate capacities. The shear stress concentration and the localization of concrete cracks near to the shear connectors also occur easily. In order to overcome these problems, a hybrid FRP-steel-concrete composite system using a wet-bonding method between the FRP and cast-in-place concrete is proposed as shown in Fig. 1. The hybrid FRP-steel-concrete composite system consists of three parts: an externally bonded hybrid FRP shell, a cast-in-place concrete core and steel rebars with very low or controlled reinforcement ratio. For the hybrid FRP shell, carbon fiber reinforced polymer sheets and EG sheets with higher ductility are used as longitudinal reinforcements in order to realize sufficient performances in stiffness, strength and ductility. Based on our previous research [8], however, we realize that the strength requirement of this kind of FRP-steel-concrete composite system can be easily met due to the high strength performance of FRP composites. The main design concerns for the proposed structures, therefore, are the stiffness and ductility requirements. High modulus type of carbon fiber reinforced polymer (MC) sheets were mainly used in this study. Outside the longitudinal reinforcement of hybrid FRP sheets, additional EG sheets with high ductility were hoop directionally wrapped as shear reinforcements. They will function specifically to confine the whole concrete core and to prevent premature debonding of interior longitudinal FRP sheets. The FRP shell was coated with bonding agents prior to concrete casting. What is important is that the hybrid shell is also able to protect the inner concrete core and steel rebars from environmental corrosion.

3 Experimental program

3.1 Details of specimens

Tensile properties of the MC, EG, and high strength type of carbon FRP (SC) applied are shown in Table 1, which refer to our previous study [9]. In this study, the following factors are investigated:
1) FRP bonding process (considering a wet-bonding method or externally bonded after curing concrete)
2) Amount of different types of FRP sheets

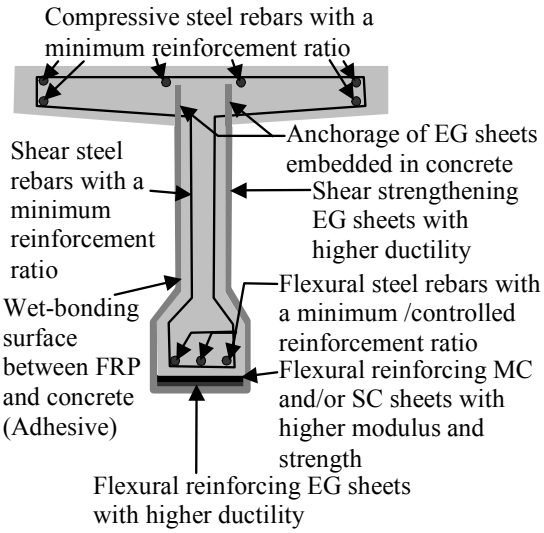

Fig.1. Concept of an FRP-steel-concrete hybrid system based on wet-bonding technology.

Table 1 Summary of mechanical properties of different fiber sheets

Type of FRP sheets	MC	SC	EG
Measured average tensile strength (N/mm^2)	2613	4232	1793
Measured average elastic modulus (kN/mm^2)	571	243	80
Calculated rupture strain (%)	0.46	1.74	2.24
Nominal thickness (mm)	0.143	0.167	0.118
Unit weight of fibers (g/m^2/1 layer)	300	300	200

3) Shapes of hybrid structures (Rectangular and T sections)
The details of all hybrid specimens are listed in Table 2. A longitudinal steel ratio (p_s) of 0.29% was chosen as a minimum value. After bonding the longitudinal FRP, four layers of EG sheets were hoop directionally wrapped. Epoxy resin was used as a matrix in all of the FRP shells. All cast-in-place concrete cores of the hybrid specimens were designed as shown in Fig. 2-5. In the proposed hybrid system, before casting the concrete, the inner surface of the FRP shells was first treated with epoxy resin in order to provide a sufficient bond layer between the fresh concrete and the FRP shell. Thus, the fiber volume content (V_f) of the hybrid FRP sheets was set as 50%, based on the JSCE guideline for repairing and reinforcing real concrete structures with externally bonded FRP sheets [10]. In the case of FRP bonding with the wet-bonding method, the concrete surface was treated with a diamond sander and painted with

Table 2 Details of FRP-steel-concrete and RC specimens

Specimens	Shape of specimen	Steel rebar for longitudinal reinforcement	Fiber sheets for longitudinal reinforcement	Steel rebar for shear reinforcement	Fiber sheets for shear reinforcement
NF-1.66%	Rectangular beam	2-D16 (1.66%)	None	21-D10	None
NF-2.39%	Rectangular beam	2-D19 (2.39%)	None	21-D10	None
1.5MC-4EG-W	Rectangular beam	3-D6 (0.29%)	1.5 layers MC + 4 layers EG	4-D10	4 layers EG
1.5MC-4EG-E*	Rectangular beam	3-D6 (0.29%)	1.5 layers MC + 4 layers EG	4-D10	4 layers EG
2MC-5EG	Rectangular beam	3-D6 (0.29%)	2 layers MC + 5 layers EG	4-D10	4 layers EG
T-NF-1.20%	T girder	2-D16 (1.20%)	None	24-D10	None
T-NF-1.73%	T girder	2-D19 (1.73%)	None	24-D10	None
T-2MC-5EG-0.29%	T girder	3-D6 (0.29%)	2 layers MC + 5 layers EG	4-D10	4 layers EG
T-2MC-6EG-0.29%	T girder	3-D6 (0.29%)	2 layers MC + 6 layers EG	4-D10	4 layers EG
T-2SC-5EG-W	T girder	2-D13 (0.77%)	2 layers SC + 5 layers EG	4-D10	4 layers EG
T-2SC-5EG-E	T girder	2-D13 (0.77%)	2 layers SC + 5 layers EG	4-D10	4 layers EG

* The hybrid FRP sheets are externally bonded after curing of concrete.

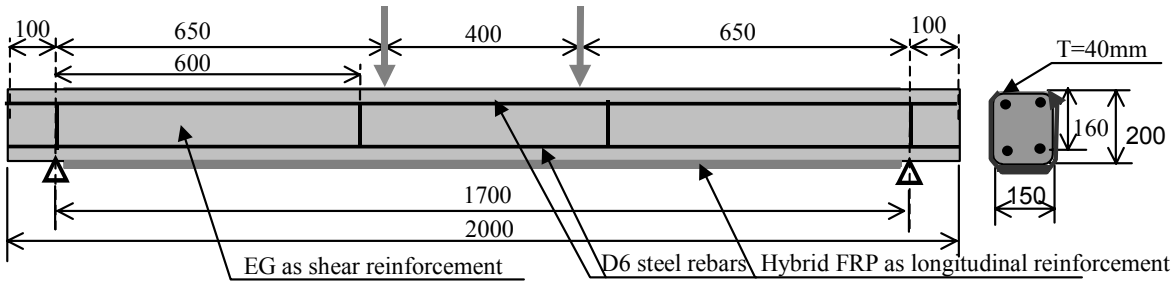

Fig.2 Details of FRP-steel-concrete hybrid beam specimens

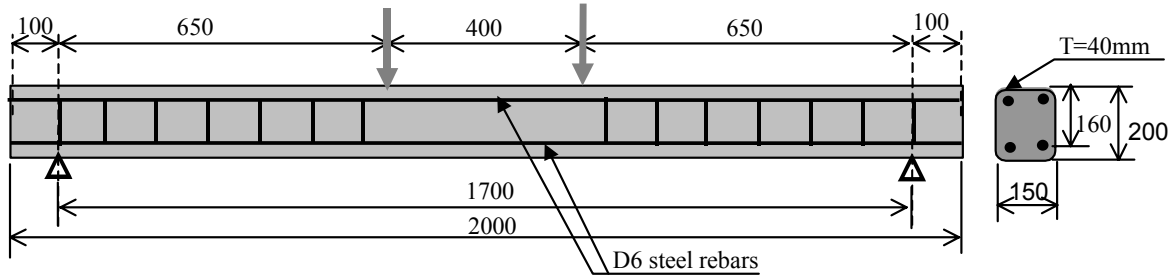

Fig.3 Details of RC beam specimens

epoxy primer. The two rectangular RC beams with p_s of 1.20% and 1.73%, and two T girders with p_s of 1.66% and 2.39% were cast as the control specimens. The average compressive strength and elastic modulus of the cast-in concrete were 29MPa and 30GPa, respectively, in the rectangular specimens, and 45.5MPa and 31GPa, respectively, in T specimens, as determined by three cylinder tests just before bending tests.

3.2 Experimental procedures

All the specimens were subjected to a 4-point bending, with a clear span and load span of 1700mm and 400mm, respectively. The specimens were loaded

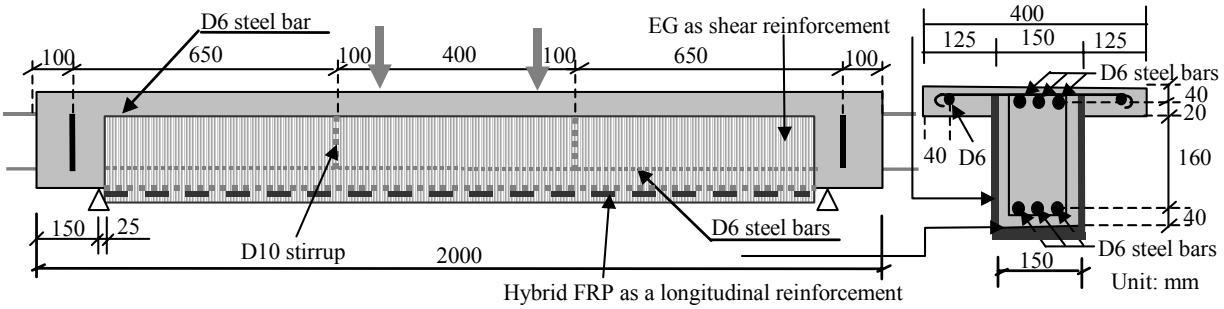

Fig.4 Details of FRP-RC hybrid T girder specimens

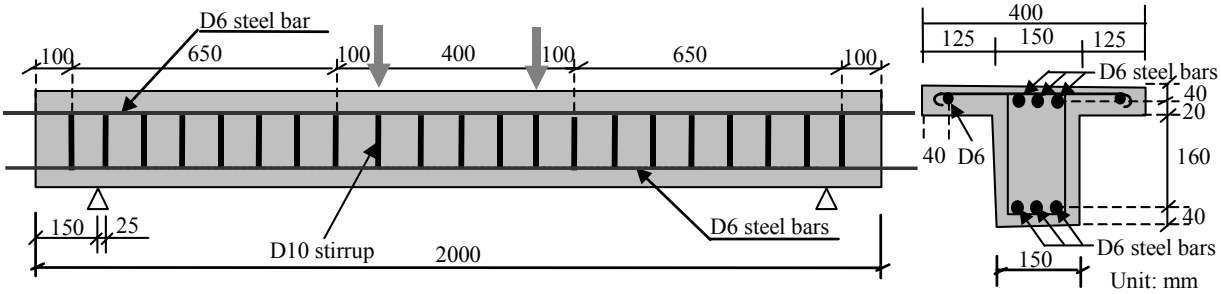

Fig.5 Details of RC T girder specimens

under a displacement control manner at a loading rate of 0.5mm/min. The specimens were instrumented to record load, deflection and strain measurements. Two linear variable displacement transducers (LVDTs) were used to record the mid-span deflection. The strains of longitudinal FRP sheets and tensile rebar under the mid-span and two loading points were individually measured with three strain gauges with a gauge length of 5mm.

4 Experimental result and discussion

4.1 Mechanical properties of the FRP-steel-concrete members

4.1.1 Feasibility of the wet-bonding method

To confirm the feasibility of the wet-bonding method, two types of specimens of both rectangular and T beams were investigated with the same type and amount of hybrid FRP sheets. The only difference was the bonding process between FRP shell and concrete. These specimens are named as 1.5M-4EG-W and T-2SC-5EG-W with wet-bonding method and 1.5M-4EG-E T-2SC-5EG-E with externally bonding after curing of concrete. Figs. 6 and 7 show the load versus mid-span displacement curves of these specimens. As for rectangular specimens, the failure occurs due to MC sheets rupture while FRP debonding occurs for T specimens with wet-bonding method were FRP debonding because of the adoption of the higher strength of the SC. As for the specimens with rectangular section no

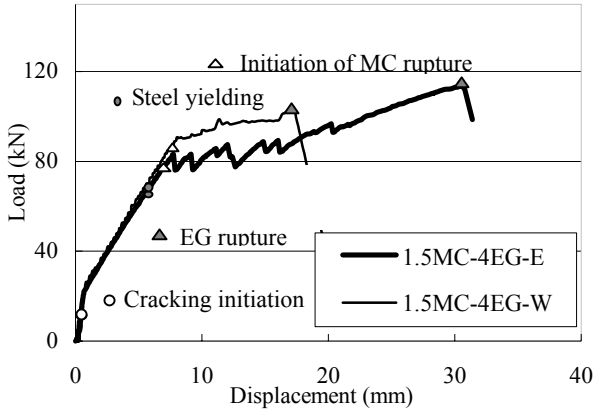

Fig. 6 Comparative results on different FRP bonding processes (Rectangular beams)

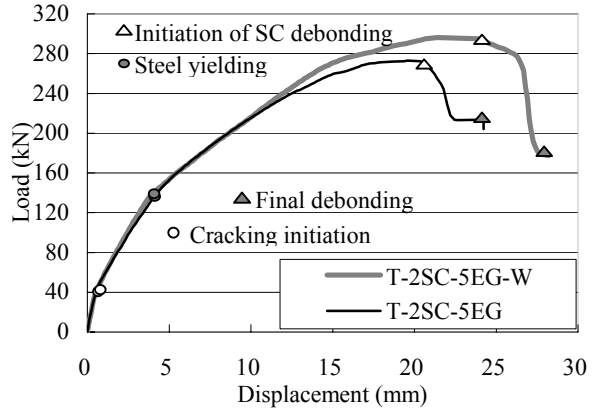

Fig. 7 Comparative results on different FRP bonding processes (T beams)

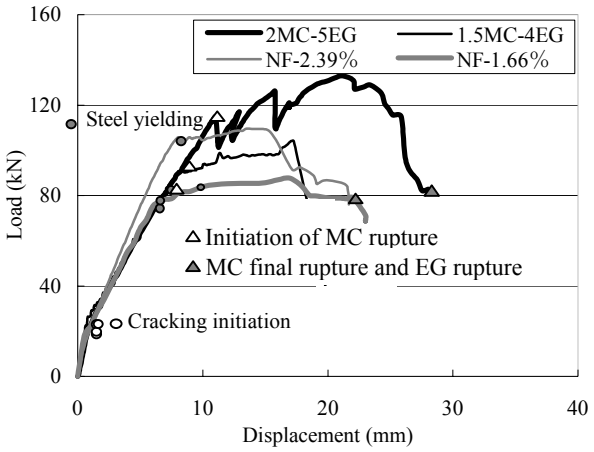

Fig. 8 Experimental result of load versus displacement relationship (Rectangular beams)

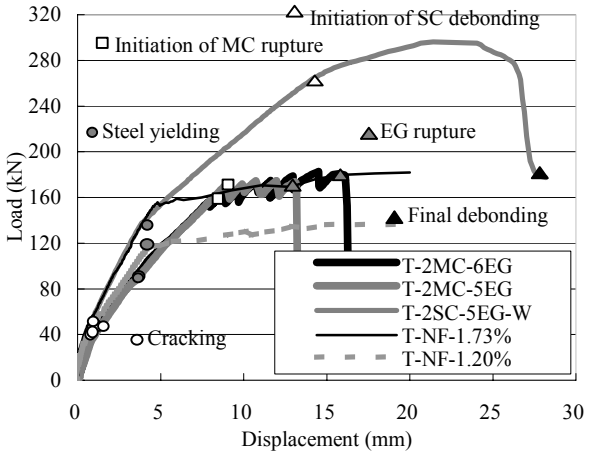

Fig. 9 Experimental result of load versus displacement relationship (T beams)

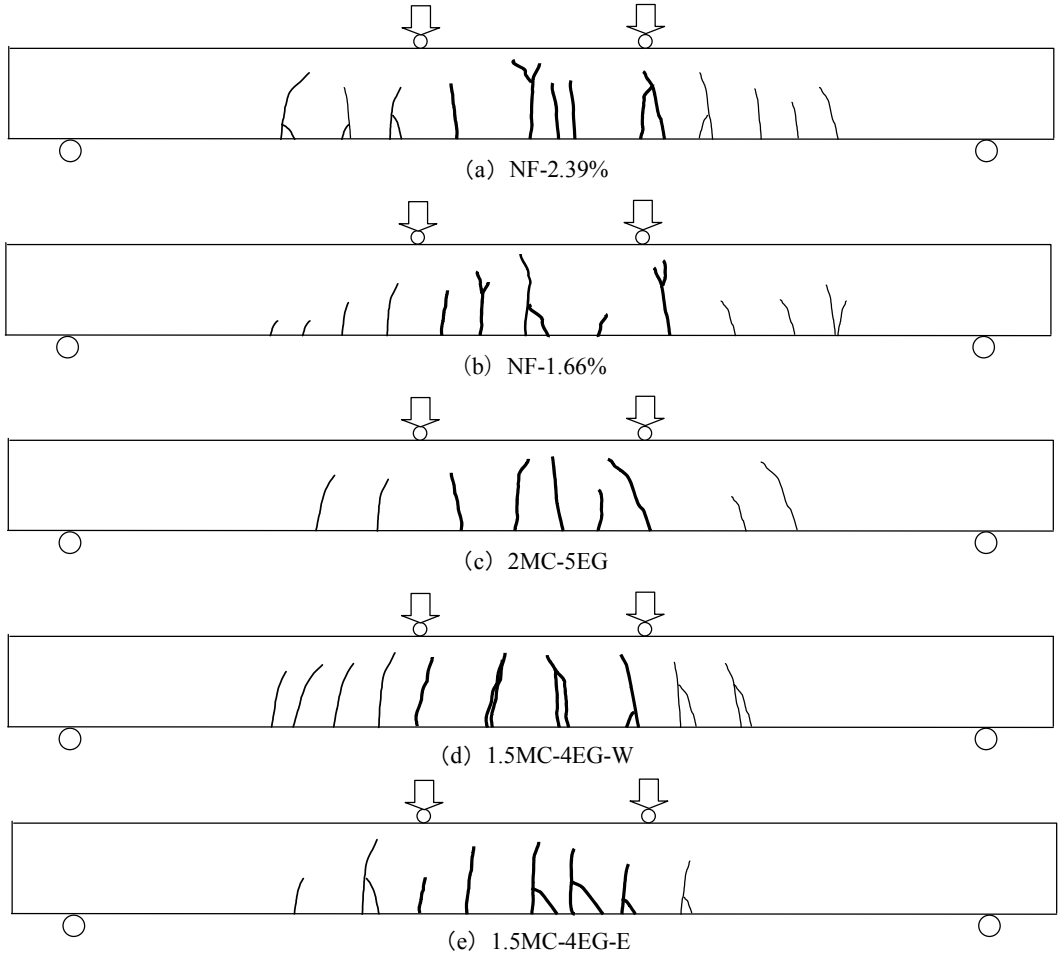

Fig. 10 Crack distributions at ultimate load for rectangular specimens

debonding occurs until the occurring of final failure due to FRP rupture. Although the 1.5MC-4EG-W specimen with wet-bonding shows lower ductility than 1.5MC-4EG-E specimen with externally bonding, a higher load carrying capacity, in reverse, is realized. The T specimens show FRP debonding failure. Comparing with external bonding after curing of concrete, the specimen with wet-bonding show higher performances on both strength and ductility. As a result, the wet-bonding method was

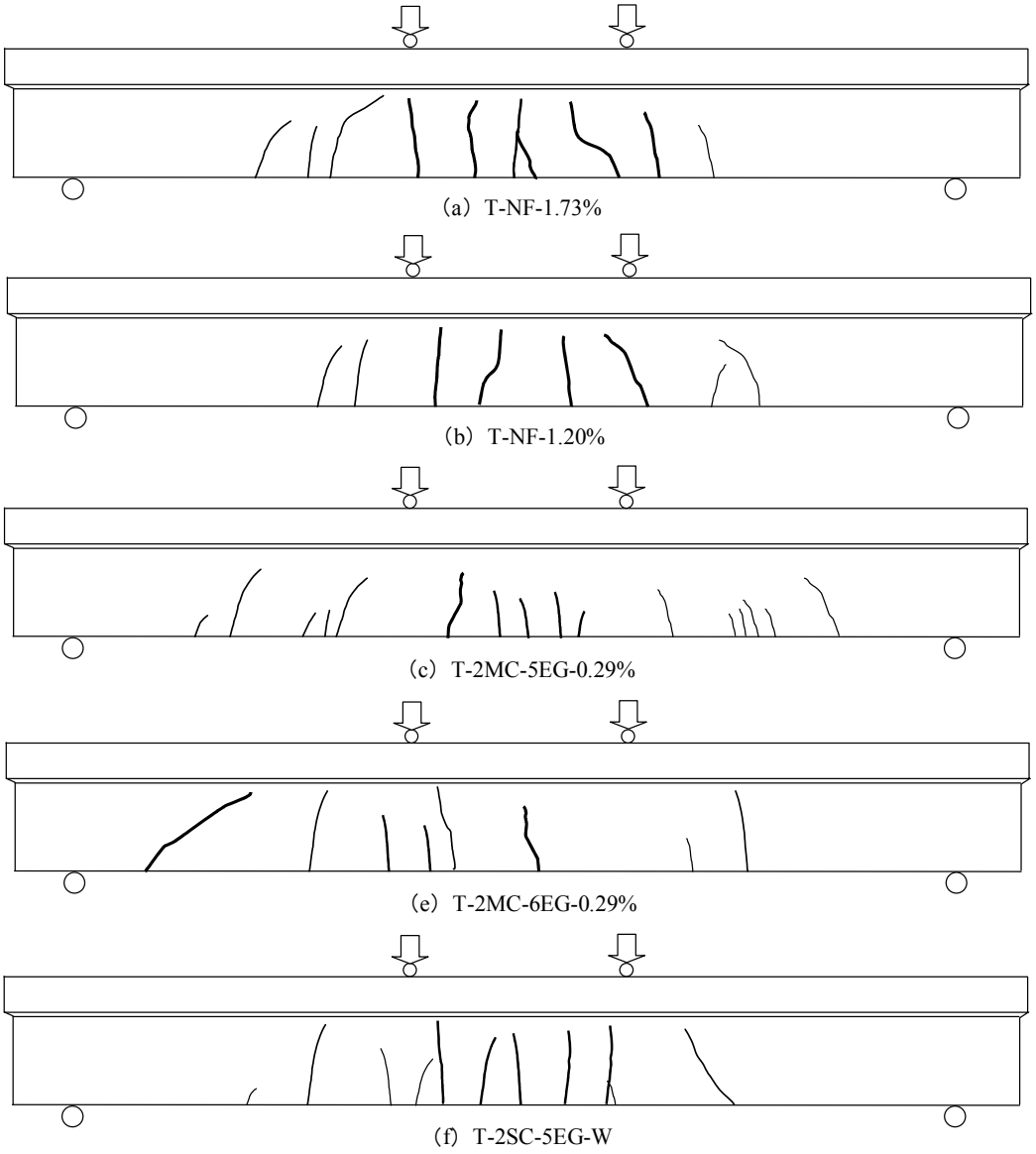

Fig. 11 Crack distributions at ultimate load for T specimens

confirmed to favor obtaining good integrative performances and a sound composite effect between the FRP and the concrete surface.

4.1.2 Flexural behavior

Fig. 8 shows the load versus mid-span displacement curves of rectangular beams with the wet-bonding method. The cracking load and steel yield load are the nearly same as or higher than those of control beams. However, the stiffness before steel yielding is lower than that of control beams. The beams failed due to the rupture of MC after steel yielding and gradual rupture. No debonding in longitudinal and axial FRP sheets was observed. Fig. 9 shows the load versus mid-span displacement curves of T beams with the wet-bonding method. The cracking load is the nearly same as or higher than those of control beams. The steel yield loads of T beams were found to be lower than those of control beams, but the loads at the initial rupture of the MC were nearly same as the steel yield load of T-NF-1.73% beam. The stiffness of T-2MC-6EG and T-2MC-5EG specimens were lower than those of control beams because the values of the p_s of the hybrid beams were smaller than those of the control beams. However, it is considered that the stiffness of T-2SC-5EG-W is higher than that of control beams with increasing the steel reinforcement ratio.

4.1.3 Crack distribution

The propagation of concrete cracks are shown in Figs. 10 and 11. The distribution of concrete cracks

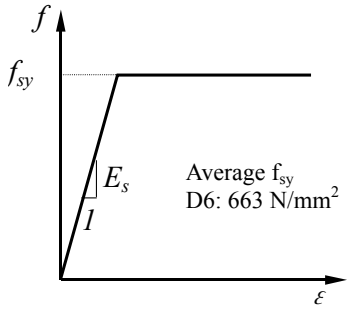

(a) Steel rebar

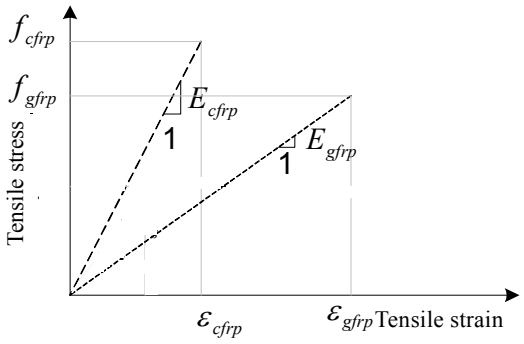

(b) FRP sheet

Fig. 12 Mechanical performances of different types of materials

is nearly same as in the control specimens. As a result, we conclude that the favorable dispersive crack pattern can be realized even at the small steel reinforcement ratio.

4.2 Theoretical investigation on the flexural properties of FRP-steel-concrete specimens

4.2.1 Mechanical performances of different types of materials

Fig. 12 shows the mechanical behaviors of different types of materials utilized in this study. According to the JSCE Standard Specifications for Design and Construction of Concrete Structures (Design) [11], the stress of steel rebars increases linearly with strain until their yielding point; after that point, the stress is maintained until the final rupture strain, as shown in Fig. 12 (a). The mechanical behavior of FRP sheets is elastic until their final failure, as shown in Fig. 12 (b). For FRP sheets, the failure takes place gradually and in an order from the fibers with a low final strain to the ones with a large final strain, and the fractured fibers will not function in reinforcing.

4.2.2 Cracking load

All materials are transformed to their equivalent concrete by using their respective modular ratios. The depth of the neutral axis can be calculated as:

$$h_c = \frac{A_c d_c + (A_{s1} d_1 + A_{s2} d_2)(n_s - 1) + A_f h (n_f - 1)}{A_{total}} \quad (1)$$

$$A_{total} = A_c + (A_{s1} + A_{s2})(n_s - 1) + A_f (n_f - 1) \quad (2)$$

Table 3 Comparison of experimental and theoretical results

Specimens	Experimental load P_{exp} (kN)			Calculated values P_{cal} (kN)		
	Cracking	Steel yielding	Initial rupture of HM	Cracking	Steel yielding	HM rupture
1.5MC-4EG-W	14.0	76.3	90.4	9.5	68.6	82.2
2MC-5EG	14.9	84.0	114.9	9.6	81.9	100.4
1.5M-4EG-E	14.2	74.1	83.3	9.5	68.6	82.2
T-2MC-5EG	21.7	120.7	160.7	20.3	125.5	152.3
T-2MC-6EG	19.8	125.8	155.8	20.3	121.9	157.1
T-2SC-5EG-W	24.4	132.9	273.0	24.1	120.8	*
T-2SC-5EG-E	24.4	133.4	296.2	24.1	120.8	*

* These values cannot be calculated because strain gauges are broken before FRP debonding.

where $n_s = \frac{E_s}{E_c}$ for rebars and $n_f = \frac{E_f}{E_c}$ for the fiber sheets, A_c and A_f are the concrete and FRP sheets cross-sectional areas, respectively. Then, the total cracking load P_{cr} can be expressed.

$$P_{cr} = \frac{2 \cdot I_g \cdot f_t}{L_2 \cdot h_c} \quad (3)$$

where I_g is the moment of inertia of the cross section before cracking; L_2 is the distance of loading from the end of the girder and f_t is the tensile strength of concrete. The experimental and calculated cracking loads are shown in Table 3. The experimental reproduction is validated due to the fact that the experimental cracking loads agree well with the calculated loads.

4.2.3 Steel yield load

To calculate the yield load, the neutral axial should be calculated first according to the equilibrium equation between the compressive force of the upper concrete and the tensile force of the steel rebars and FRP sheets. The compressive rebars may be negligible during the calculation of neutral axial according to the JSCE Standard Specifications for Design and Construction of Concrete Structures (Design) [11]. Then, the flexural moment of inertias of rebars and FRP sheets are decided to relative to neutral axial, and they are transferred into loads. Finally, the yielding load of the FRP-steel-concrete structures can be calculated according to the yielding stress of the rebars and the stress carried by the FRP sheets at the yield of rebars. The experimental and calculated yielding loads of the FRP-steel-concrete specimens are listed in Table 3. The experimental loads do agree well with the calculated ones for the specimens with FRP rupture mode.

4.2.4 MC rupture load

The MC rupture load is calculated with the method proposed by the authors in previous study [12], which is given according to the following equation in terms of MC rupture strain (ε^*_{fc}).

$$M_u = f_y A_s (d - y) + E_{fc} \varepsilon^*_{fc} A_f (h - y) \quad (4)$$

where f_y is yielding strain of the steel reinforcements, As the total area of cross-section, d the distance from upper side of the structure to tensile rebars, $y = \beta_1 x/2$ (β_1=0.8 according to Standard Specifications for Design and Construction of Concrete Structures (Design) [11]), x the distance from neutral axial to upper side of the girder, E_{fc} the elastic modulus of FRP sheets, A_f the area of cross-section of FRP sheets. M_u can be calculated in terms of the experimental maximum load. The experimental and calculated maximum strains of the FRP sheets are listed in Table 3. It is apparent that the experimental loads agree well with the calculated ones.

5 Conclusions

This study aimed at developing innovative FRP-steel-concrete structures with excellent corrosion resistance and integrative structural performances. Both experimental and theoretical studies were carried to characterize the properties of the proposed structures. According to the investigation, we can conclude the following:

(1) The wet-bonding method was confirmed to favor obtaining a good integrative property and a sound composite effect between the FRP and the concrete surface.
(2) Compared to RC structures, an integrative structural performances of FRP-steel-concrete structures can be realized, including load carrying capacity, steel yield load and ductility; however, the stiffness of the hybrid beams should be improved further.
(3) It is noted that the favorable dispersive crack distribution can be realized even at the FRP-steel-concrete beam with a very low steel reinforcement ratio.
(4) The flexural properties of FRP-steel-concrete structures can be evaluated according to the existing bending theories. The good agreement between experimental results and theoretical results reveals the reproducibility of the experiments.

Acknowledgement

The authors gratefully acknowledge the cooperation of Nittetsu Composite Co. Ltd., Japan for providing carbon fiber sheets and epoxy materials.

References

[1] Descovic N., Triantifillou T.C. and Meier U., “Innovative design of GFRP combined with concrete: short term behaviour”, ASCE Journal of Structural Engineering, 121, 7, pp 1069-1078, 1995
[2] Fam A. and Rizkalla S., “Flexural behavior of concrete-filled fiber-reinforced polymer circular tubes”, ASCE Journal of Composites for Construction, 6, 2, pp 123-132, 2002

[3] Sekijima K., Ogisako E., Miyata K. and Hayashi K., "Analytical study on flexural behavior of GFRP-concrete composite beam", 1st International Conference on FRP Composites in Civil Engineering (CICE 2001), J.G. Teng, Hong Kong, China, 2, pp 1363-1370, 2001

[4] Thomas K., Herbert G., "Design of hybrid bridge girders with adhesively bonded and compositely acting FRP deck " Composite structures, 74, 2, pp 202-212, 2006

[5] Ribeiro M., Tavares C., Ferreira A. and Marques A., "Static flexural performance of GFRP-polymer concrete hybrid beams", 1st International Conference on FRP Composites in Civil Engineering (CICE 2001), J.G. Teng, Hong Kong, China, 2, pp 1355-1362, 2001

[6] Shao Y., Nemes J., Yeats M. and Loblick G., "GFRP-concrete flooring deck", 3rd International Conference on Advanced Composite Materials in bridges and Structures, CSCE, Ottawa, Canada, pp 161-168, 2000

[7] Black S., "Hybrids of composite and concrete make cost-effective bridge decks", Composites Technology, Ray Publishing, Wheat Ridge, USA, pp 20-25, 2004

[8] Wu, Z.S., Li, W. and Sakuma, N., "Innovative externally bonded FRP/concrete hybrid flexural members", Elsevier Journal of Composite structures, 72, 3, pp 289 -300, 2006

[9] Z.S. Wu, K. Sakamoto, K. Iwashita, Q. Yue "Hybridization of continuous fiber sheets as structural composites". Journal of the Japan Society for Composite Materials, Vol.32, No.1, pp.12-21, 2006

[10] Japan Society of Civil Engineers "Recommendations for Upgrading of Concrete Structures with Use of Continuous Fiber Sheets". Concrete Engineering Series 41, 2001

[11] JSCE, "Standard Specifications for Design and Construction of Concrete Structures (Design). 1996

[12] Wu Z.S., Matsuzaki T. Fukuzawa K.and Kanda T., "Strengthening Effects on RC Beams with Externally Prestressed Carbon Fiber Sheets". Journal of Material, Concrete Structures and Pavements, JSCE, pp.153-165, 2000